https://doi.org/10.5194/egusphere-2026-3223
Preprint. Discussion started: 6 July 2026

Freshwater forcing along the Indian Coastal Seas: Impacts on Productivity and Acidification

Kunal Madkaiker[1], Ambarukhana D. Rao[1], Vimlesh Pant[1], Jonathan M. Lauderdale[2]

[1]Centre for Atmospheric Sciences, Indian Institute of Technology Delhi, New Delhi, India
[2]Department of Earth, Atmospheric and Planetary Sciences, Massachusetts Institute of Technology, Cambridge, Massachusetts, USA

Correspondence to: Kunal Madkaiker (Kunal.Ajit.Madkaiker@cas.iitd.ac.in)

Abstract. Freshwater fluxes from precipitation and river runoff play a critical role in modulating upper-ocean stratification, nutrient availability, and biogeochemical processes in the coastal waters of the Indian subcontinent. The formation of the barrier layer thickness (BLT) links freshwater input to vertical mixing, influencing both productivity and carbonate chemistry. High-resolution (5 km) MITgcm-BLINGv2 simulations are conducted for the Arabian Sea (AS) and the Bay of Bengal (BoB), and sensitivity experiments are performed to represent reduced and increased freshwater perturbations. We analyzed seasonal variability of buoyancy frequency (N^2), mixed layer depth (MLD), net primary productivity (NPP), pH, and phytoplankton biomass across five coastal regions. Reduced freshwater scenarios weakened or eliminated BLT, leading to deeper MLD and N^2 maxima, with subsurface nutrient-rich waters entrained upward. This enhanced nutrient availability increased NPP in the coastal regions. However, the upward transport of subsurface carbon also lowered surface pH by 0.03, indicating a trade-off between biological enhancement and increased surface acidification. In the increased freshwater scenario, the BLT strengthened, the MLD shoaled, and NPP decreased, while surface pH increased due to reduced vertical carbon exchange. Interestingly, stratification deepening under reduced freshwater input is more pronounced in the southeastern AS than in the BoB, contrasting conventional understanding. Vertical phytoplankton responses are consistent with these trends, with small and large phytoplankton biomass increasing under weaker BLT and decreasing under enhanced BLT. Freshwater-driven BLT modulation drives a complex interplay between carbon uptake and export along Indian coastal waters. These findings emphasize the importance of accurately representing freshwater fluxes in biogeochemical models to capture regional ecosystem responses.

1 Introduction

The coastal regions of the north Indian Ocean (NIO), encompassing the Arabian Sea (AS) and the Bay of Bengal (BoB), experience strong seasonal variability driven by wind and freshwater forcings. Freshwater inputs from the South Asian monsoon and large river discharges strongly influence the salinity structure, stratification, and exchange between coastal and open-ocean waters (Kumar et al., 2002; Schott et al., 2009). Understanding how freshwater influences the state of the coastal waters is important for predicting biological responses under a changing climate. Freshwater input into the region originates

https://doi.org/10.5194/egusphere-2026-3223
Preprint. Discussion started: 6 July 2026

from two primary sources: direct precipitation and river discharge. The Indian Summer Monsoon (ISM) is the dominant driver of seasonal precipitation, contributing significantly to surface freshwater input between June and September. However, projections of future monsoon behaviour remain uncertain. Some climate models predict strengthening of the ISM with ~10% more rainfall under a warming scenario (Katzenberger et al., 2022; Maharana et al., 2020; Sahastrabuddhe et al., 2023), while others suggest a weakening or delayed onset (Naidu et al., 2009, 2015; Paul et al., 2016). These discrepancies pose major challenges for anticipating changes in oceanic salinity and stratification patterns.

The BoB receives most of its freshwater load from major Himalayan-fed rivers such as the Ganga, Brahmaputra, and Irrawaddy. Observational studies have documented a significant freshening of the BoB surface waters over the past two decades, primarily attributed to increased glacial melt and precipitation over the basin (Goes et al., 2020; Sridevi and Sarma, 2021). Such changes have implications for the physical and biogeochemical structure of the region, influencing the vertical exchange of heat, salt, and nutrients. In contrast, the AS receives relatively less freshwater input and is influenced more by open-ocean processes and lateral exchange through monsoon-driven circulation. River discharge trends are also highly uncertain due to human interventions such as dam construction, water diversion, and land-use changes. Several recent studies suggest that damming activities could reduce the net freshwater input to coastal regions, especially in the BoB, by trapping upstream river runoff (Acharyya et al., 2012; Boulange et al., 2021). This could counteract the freshening effects of glacier melt and monsoonal intensification, leading to complex, regionally varying outcomes.

Such opposing influences, which can either increase or decrease freshwater input, highlight the need to improve our understanding of freshwater variability in the NIO and its implications for coastal ocean biogeochemistry. Freshwater-driven changes in salinity and stratification influence vertical mixing and lateral advection, which in turn regulate the residence time of surface waters, nutrient supply, phytoplankton growth, and air-sea CO_2 exchange (Jayaram et al., 2021; Resplandy et al., 2012). These processes are important in the context of ocean acidification, where modulation in dissolved inorganic carbon (DIC) and alkalinity (ALK) concentrations, and the Revelle factor, determine the buffering capacity of the ocean against rising atmospheric CO_2.

Despite advances in satellite observations and *in situ* measurements, key uncertainties remain in quantifying the impact of freshwater variability on productivity and carbon cycling in these regions. These uncertainties arise from a limited spatial coverage of observational networks, coarser resolution of global models, and the nonlinear interaction between freshwater fluxes, stratification, nutrient cycling, and biological feedback. Recent modelling efforts have begun to address these gaps using high-resolution physical-biogeochemical models, which can resolve mesoscale features and simulate the fine-scale variability in biogeochemical properties (Chakraborty et al., 2022; Valsala and Maksyutov, 2010).

https://doi.org/10.5194/egusphere-2026-3223
Preprint. Discussion started: 6 July 2026

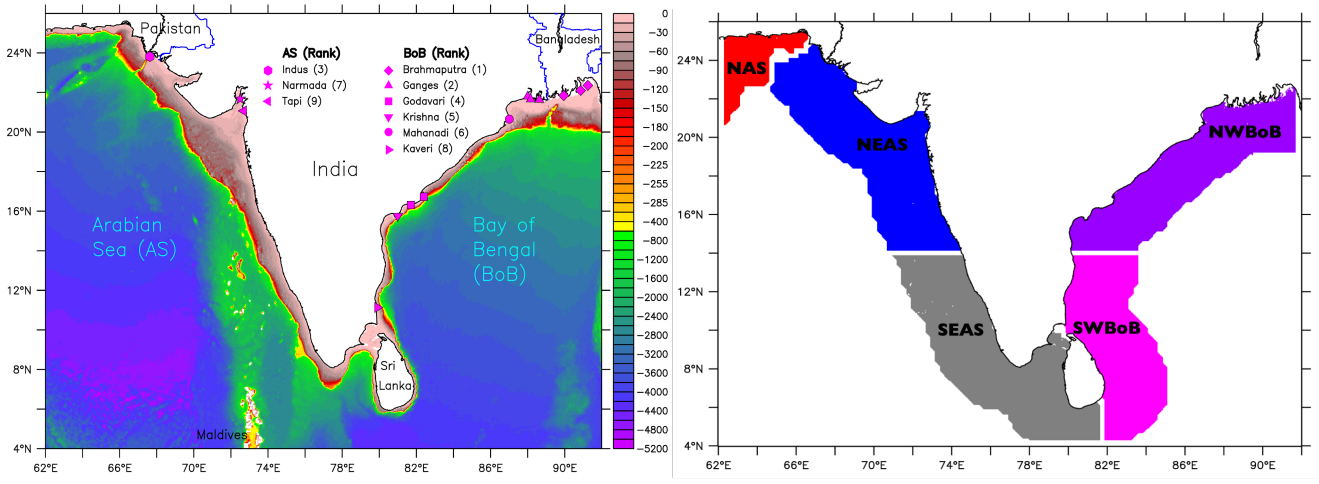

Figure 1. (Left) study area. The colour scale represents bathymetry (in m). The locations of river mouths for major Indian subcontinental rivers are marked with purple symbols. The rivers are sorted by their discharge volume and basin. (Right) Coastal masks obtained from Resplandy et al. (2024) and divided into five subregions.

In this study, we use a high-resolution (~5 km) regional configuration of the MITgcm, integrated with its BLINGv2 biogeochemical model, to understand the influence of freshwater variability on coastal waters along the Indian coast (refer to Fig. 1). This model configuration includes key carbon and nutrient tracers (DIC, ALK, nitrate, phosphate, and iron) and three phytoplankton classes. We assess particularly the relationship between freshwater-driven changes in stratification and their influence on productivity and ocean acidification. Specifically, we address the following questions:

1. How do the implications of freshwater variability alter the physical state (e.g., salinity, stratification) of the coastal waters in the AS and BoB?

2. How does the change in the physical state of the waters influence biological productivity and seawater acidity in these regions?

By answering these questions, we aim to improve our understanding of freshwater-biogeochemical interactions in the NIO and to provide insights for predicting future changes under an evolving climate and anthropogenic forcing. The structure of this study is as follows: Sect. 2 presents the model configuration, the datasets used, and the methodology. Section 3 covers the results, Sect. 4 follows the discussion, and Sect. 5 presents the conclusions.

https://doi.org/10.5194/egusphere-2026-3223
Preprint. Discussion started: 6 July 2026

2 Model, Data and Methods

2.1 Model description (MITgcm-BLINGv2)

We employ the MITgcm (Marshall et al., 1997) model, which is set up along the coastal waters of the Indian subcontinent, including the AS and the BoB (refer to Fig. 1). The model domain spans 4°-26°N and 62°-92°E, allowing the simulation to resolve cross-basin exchanges between the AS and the BoB. A spatial resolution of 5 km was selected to allow the setup to be eddy-resolving. The configuration followed a z-coordinate vertical system with 49 levels and a maximum depth of 4500 m. The remaining aspects of the physical configuration, including bathymetry, numerical schemes, boundary conditions, atmospheric forcing, and model initialization, followed Madkaiker et al. (2024). To avoid repetition, only elements that are directly relevant to or differ from that configuration are described here. To account for the impact of river runoff from the glacial and peninsular rivers in India, climatological discharge from Dai and Trenberth (2002) is supplied as a point source. River salinity is set to 0 psu, and river temperature is set to the ambient SST at the discharge point. At the surface, the model temperature and salinity are relaxed using monthly climatology every thirty days, based on the satellite-derived MUR SST (Chin et al., 2017) and SMAP SSS (Tang et al., 2017).

The Biogeochemistry with Light, Iron, Nutrients, and Gases version two (BLINGv2) is an intermediate-complexity module that simulates key biogeochemical processes, including nutrient cycles, phytoplankton growth, and oxygen dynamics (Galbraith et al., 2010; Verdy and Mazloff, 2017). In addition to nitrate, phosphate, silicate, and iron cycling, BLINGv2 introduces a nitrogen cycle with nitrogen fixation and denitrification. Iron limitation is reformulated to better align with phosphate limitation. Phytoplankton biomass is treated as a non-advected or diagnostic tracer, allowing for nutrient uptake calculations without assuming perfectly balanced growth. This formulation allows greater flexibility in simulating growth under light or nutrient limitation, as uptake and biomass are decoupled. The model includes three phytoplankton functional types: small phytoplankton (SP; coccolithophores), large phytoplankton (LP, diatoms requiring silicate), and diazotrophs, which compete for light and nutrients using Monod-type growth functions, modulated by temperature and irradiance. Light limitation accounts for both instantaneous and smoothed irradiance fields, representing phytoplankton exposure within the mixed layer and their photoadaptation timescale, following a γ-irradiance relaxation scheme. Chl is computed diagnostically using a fixed or variable Chl-to-carbon (Chl: C) ratio, thereby improving simulations of ocean colour and primary productivity (Verdy and Mazloff, 2017). The Chl: C ratio is influenced by Fe availability, which modifies photosynthetic antennae efficiency, linking micronutrient status to light utilization capacity. The model also incorporates simplified, community-averaged food web processes in the euphotic zone, following empirical relationships from Dunne et al. (2005), without explicitly simulating zooplankton or detritus. Organic matter is partitioned into sinking and recycled pools using a temperature-dependent scheme. Oxygen consumption occurs during remineralization, and surface gas exchange is computed using OCMIP2 protocols and a wind-speed dependent parameterisation (Wanninkhof, 1992). The initial and boundary

https://doi.org/10.5194/egusphere-2026-3223
Preprint. Discussion started: 6 July 2026

forcings for tracers are based on the monthly climatology of Broullón et al. (2019, 2020) and include dissolved iron data from the Copernicus Marine Environment Monitoring Service's (CMEMS) Global Ocean Biogeochemistry Hindcast dataset (GLOBAL_MULTIYEAR_BGC_001_029). The atmospheric components of pCO2 are taken from Andrews et al. (2014) and iron dust from Hamilton et al. (2019), following a pentad climatology. The iron dust is included to account for micronutrient limitation. The effect of iron deposition is indirectly captured in the biological production term. Riverine nutrient inputs are incorporated at the river discharge locations. Following Dunne et al. (2020), a constant phosphate concentration is prescribed and scaled by river discharge volume. Nitrate and carbon riverine concentrations are then derived using the stoichiometric ratio of C: N: P (106:16:1). BLINGv2 has been used in several studies (Mazloff et al., 2010; Swierczek et al., 2021; Twelves et al., 2024; Verdy and Mazloff, 2017) for studying productivity patterns, carbon fluxes, and iron limitations. The physical and biogeochemical model configuration relies on climatological forcing fields computed based on data from the last two decades (2001-2020) to represent the mean state of the ocean.

The physical model is initialized with a warm start to minimize the spin-up time and computational cost. It is then integrated for six years using the climatological forcing fields. From the 7th year onwards, the BLINGv2 is included in the integration and run for one more year. The 8th year of simulation is then used for analysis. By the end of the spin-up period (7th year), the model has reached a mean steady state, allowing us to analyze the surface plankton and nutrient dynamics based on the input climatological forcings.

2.2 Observational datasets

To validate the model-simulated SSS, we used the Soil Moisture and Ocean Salinity (SMOS) SSS v8.0 level 3 (Boutin et al., 2023) and the gridded Coriolis Ocean Dataset for Reanalysis (CORA) v5.2 (Szekely et al., 2019) datasets. SMOS uses an improved debiasing technique and is available at a spatial resolution of 0.259° × 0.196°. CORA v5.2 data have been produced using multiple *in situ* sampling techniques, including Argo floats, drifters, gliders, and moorings. It has a spatial resolution of 0.5°, with data available from the surface to 2000 m depth.

2.3 Methods

We conducted one control simulation (CTRL) and four freshwater-sensitivity experiments (SENS1-SENS4) to examine how excess or deficit freshwater forcing alters the biogeochemical state of coastal waters adjoining the Indian subcontinent. The CTRL simulation represents the reference case, while each sensitivity experiment selectively removes or enhances freshwater sources.

CTRL*: Default simulation.*

SENS1*: No precipitation (river runoff retained).*

SENS2*: No river runoff (precipitation retained).*

SENS3*: No precipitation and no river runoff.*

https://doi.org/10.5194/egusphere-2026-3223
Preprint. Discussion started: 6 July 2026

SENS4: *Excess freshwater forcing*, precipitation increased by 100%, and runoff from three glacial rivers (Indus, Ganga, Brahmaputra) increased by 12%, 27%, and 8%, respectively (refer to supporting information Fig. S1, S2 and S3).

The freshwater perturbations in SENS4 are not designed as direct projections of future conditions but as a 'stress-test' to explore the sensitivity of the system under upper-limit forcing. The choice of doubling precipitation reflects the high end of climate model projections for intensified regional monsoon rainfall (supporting information Fig. S1; Katzenberger et al., 2022; Maharana et al., 2020). Similarly, the scaling of glacial river runoff follows glacier-melt contributions reported in IPCC AR6 (supporting information Fig. S2; IPCC, 2023; Lutz et al., 2014). By testing these upper bounds, we aim to assess how extreme freshwater changes may affect stratification, nutrient supply, and biogeochemical cycling, rather than representing specific future projections.

The study region covers the coastal waters of the NIO adjoining the Indian subcontinent. To delineate this domain, we adopt the coastal mask defined by Resplandy et al. (2024), which extends about 300 km offshore or up to the 1000 m isobath, whichever is farther from the coast. This definition broadly encompasses shelf and slope waters and corresponds approximately to India's Exclusive Economic Zone (EEZ). The choice of this mask is motivated by two factors: (i) it captures the key regions influenced by coastal processes such as upwelling, downwelling, and river plume dynamics, and (ii) it broadly covers India's EEZ, making it directly relevant for the regional management.

The coastal mask is subdivided into five subregions based on distinct hydrographic characteristics (Fig. 1). These are the northern AS (NAS), northeastern AS (NEAS), southeastern AS (SEAS), southwestern BoB (SWBoB), and northwestern BoB (NWBoB). The division at 14° N latitude separates the northern and southern sections of each basin, as no major rivers discharge south of this latitude. The NAS and NEAS are characterized by strong winter convective mixing and nutrient entrainment associated with offshore influence of the Oman and Somalia coastal upwelling during the summer monsoon (Madhupratap et al., 1996; Wiggert et al., 2006). The SEAS experiences intense summer monsoon coastal upwelling, driven by alongshore winds and Ekman transport (Shankar et al., 2002; Smitha et al., 2008). In contrast, the SWBoB is primarily a downwelling regime during the summer monsoon but can experience weak upwelling under specific wind conditions (Vinayachandran et al., 2020). The NWBoB is strongly influenced by freshwater discharge from major rivers, which generate buoyant plumes that extend along the northern and northwestern coastal waters (Akhil et al., 2014; Sengupta et al., 2006). We use two complementary metrics to assess changes in upper-ocean stratification: barrier layer thickness (BLT) and the Brunt-Vaisala frequency (N^2). BLT is the difference between the isothermal layer depth and the mixed layer depth (Felton et al., 2014). N^2 is given as:

$$N^2 = \frac{-g}{\rho}\frac{d\rho}{dz} \quad (1)$$

where g is the acceleration due to gravity (m s^{-2}), and ρ is the potential density of seawater (kg m^{-3}). BLT quantifies the thickness of the salinity-stratified layer formed by freshwater inputs, indicating the extent to which salinity inhibits vertical mixing. In contrast, N^2 provides a local measure of water-column stability by quantifying the vertical density gradient.

https://doi.org/10.5194/egusphere-2026-3223
Preprint. Discussion started: 6 July 2026

Together, BLT describes the vertical extent of freshwater-induced salinity stratification, while N^2 characterizes the strength of the resulting density stratification.

3 Results

3.1 Surface salinity response to freshwater forcing

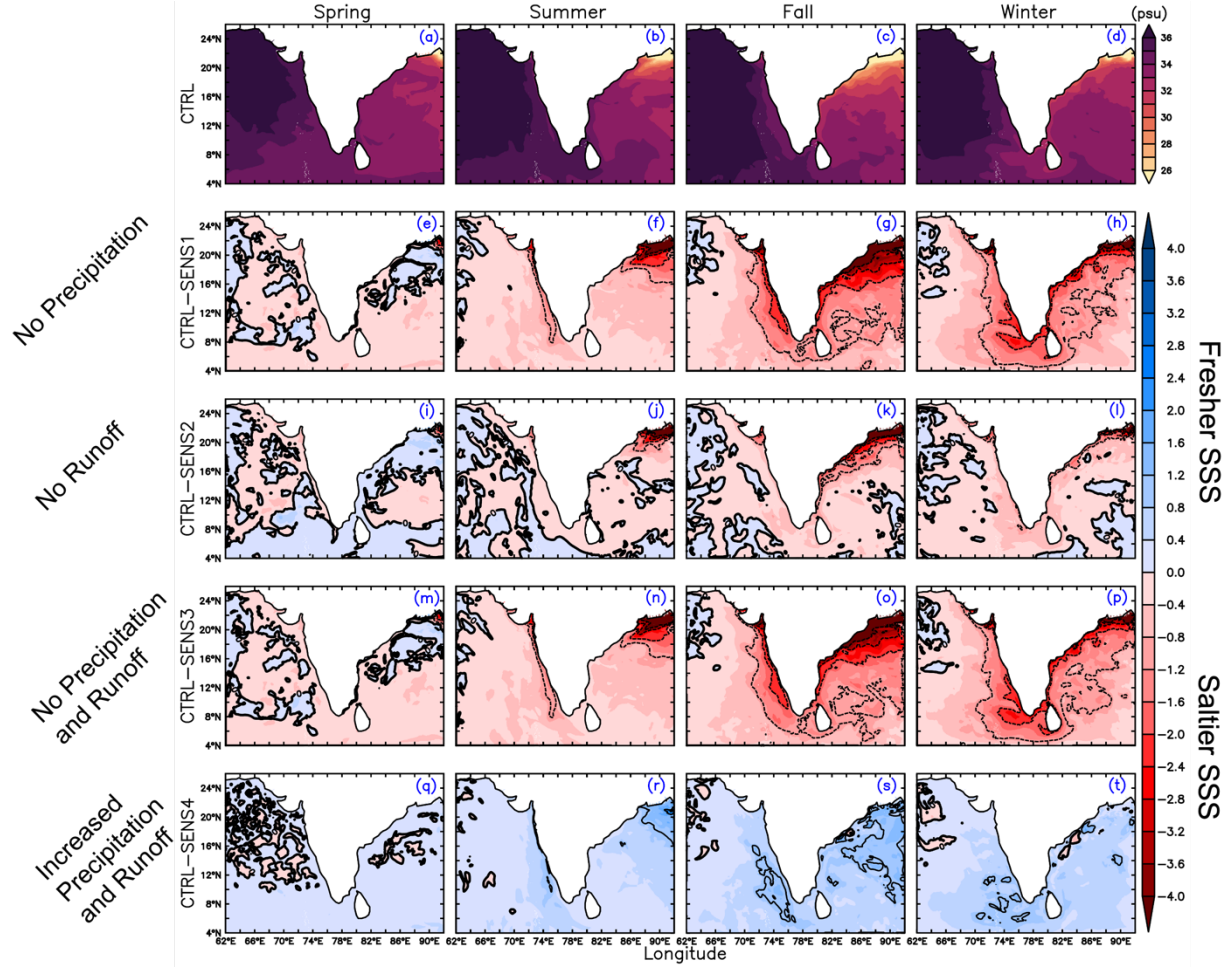

Figure 2. Seasonal climatology of SSS (in psu). Panels (a-d) show the CTRL experiment, while panels (e-h), (i-l), (m-p), and (q-t) show the SSS bias relative to CTRL for the SENS1, SENS2, SENS3, and SENS4 runs, respectively. Negative (positive) values in red (blue) denote an increase (decrease) in salinity relative to CTRL.

The seasonal distribution of sea surface salinity (SSS) in the CTRL run (Fig. 2a-d) shows strong spatial and temporal contrasts between the AS and the BoB. The AS exhibits generally high salinity (>36 psu) throughout much of the basin, with slightly lower values (~34-35 psu) along the eastern coastal waters influenced by monsoonal processes. In contrast, the BoB

https://doi.org/10.5194/egusphere-2026-3223
Preprint. Discussion started: 6 July 2026

shows much lower surface salinity (typically <33 psu), with the lowest values confined to the northern and northwestern coastal zones, consistent with the influence of freshwater discharge from the Ganga and Brahmaputra River system and local precipitation (Akhil et al., 2014; Chaitanya et al., 2014). These gradients are consistent with satellite-based SSS retrievals (Fournier et al., 2017), confirming that the model captures the state of the ocean across both basins. Furthermore, CTRL SSS has been statistically validated against observational datasets (refer to supporting information: Text S1 and Fig. S4), confirming that the model is able to capture basin-scale salinity features. The model has also been thoroughly validated for temperature and ocean currents, as detailed in Madkaiker et al. (2024).

The bias plots (CTRL-SENS; Fig. 2e-t) reveal the contribution of individual freshwater components. The second to fourth rows (SENS1 to SENS3) predominantly show negative bias (red shading), indicating that salinity in these runs is higher than in CTRL (i.e., SENS > CTRL). This suggests that the freshwater forcing components excluded or modified in these runs, particularly precipitation, play a dominant role in reducing SSS in the full run. The strong negative bias over large parts of the BoB and the eastern AS during summer and fall indicates that precipitation has a basin-wide impact, extending its influence even into regions far from the core precipitation zones (refer to Fig. 2e-h and supporting information Fig. S1). This is consistent with earlier studies showing that monsoon precipitation and associated surface runoff significantly freshen the upper ocean and increase vertical stratification (Akhil et al., 2020; Vinayachandran and Kurian, 2007). The effect of river runoff (Fig. 2i-l) appears more localized, with freshening signals in the northern BoB disappearing, and a strong negative anomaly (>3 psu) emerges along the eastern coast of India. Several regional modelling studies have reported this localized imprint of runoff on SSS (Behara and Vinayachandran, 2016; Papa et al., 2012), highlighting that riverine influence is restricted to nearshore zones due to limited horizontal spreading and strong density stratification. Figure 2m-p shows the most salinification, with widespread increase of 1-4 psu across the BoB and the AS. The similarity of the bias pattern to Fig. 2e-h suggests that when freshwater flux is considered a combined contribution from precipitation and river discharge, precipitation exerts a stronger and more widespread influence on SSS.

Figure 2q-t exhibits a positive bias (blue shading), particularly during summer and fall, implying that CTRL SSS > SENS4 SSS, i.e., the SENS4 run is fresher than CTRL. It shows widespread freshening across both basins. The strongest positive anomalies (up to 1.6 psu) occur along the northern BoB, corresponding to intensified river discharge and increased precipitation. Moderate freshening (~1 psu) is also evident in the eastern AS, suggesting that increased coastal precipitation can propagate freshwater anomalies westward through alongshore currents and eddy-driven mixing (Behara et al., 2019). The pattern aligns with the seasonal cycle of freshwater flux, which peaks during the summer, and supports previous findings that freshwater accumulation during this period controls upper-ocean stratification and mixed-layer dynamics across the NIO (Akhil et al., 2014; Sengupta et al., 2016). The magnitude and spatial extent of freshening in SENS4 demonstrate the basin's strong sensitivity to freshwater perturbations, particularly in the BoB, where persistent salinity stratification favours a stronger near-surface response to freshwater forcing (Thangaprakash et al., 2016). Overall, the pattern of SSS

https://doi.org/10.5194/egusphere-2026-3223
Preprint. Discussion started: 6 July 2026

anomalies across the experiments highlights that precipitation controls basin-scale gradients. In contrast, river runoff exerts a dominant local influence near major discharge points and coastal zones. The consistent freshening signal along the western Indian coast further suggests secondary influence from coastal catchments, where intense precipitation and land drainage deliver freshwater into the nearshore AS (Behara et al., 2019).

3.2 Barrier Layer Thickness (BLT) response to freshwater forcing

In the CTRL run (supporting information Fig. S5, a-d), the BLT exhibits strong spatial and seasonal variability, with the thickest layers occurring during the fall and winter seasons, particularly along the NWBoB and SEAS. This pattern is consistent with earlier observational and modelling studies, which have attributed the BLT formation to the input of freshwater from precipitation and river systems, together with the associated haline stratification (Durand et al., 2007; Shankar et al., 2015; Sprintall and Tomczak, 1992; Thadathil et al., 2007). In contrast, the AS shows relatively shallow BLT, with almost no BLT (shown in white colour, supporting information Fig. S5) over much of the northern and central AS, likely linked to intense upwelling and mixing (Durand et al., 2007; Thadathil et al., 2008).

	SENS1	**SENS2**	**SENS3**	**SENS4**
Spring	-3.65%	0.91%	-3.89%	3.07%
Summer	-25.80%	-2.59%	-25.92%	10.07%
Fall	-47.02%	-2.86%	-49.36%	8.05%
Winter	-26.21%	-1.74%	-26.63%	7.32%

Table 1. Seasonal percentage change in the spatial extent of BLT in the SENS experiments relative to CTRL. Negative (positive) values indicate a decrease (increase) in the spatial extent of BLT relative to CTRL.

https://doi.org/10.5194/egusphere-2026-3223
Preprint. Discussion started: 6 July 2026

The SENS experiments reveal a clear dependence of BLT on freshwater forcing (supporting information, Fig. S5e-t). The percentage changes reported in Table 1 are calculated from the number of grid cells with positive BLT values (BLT > 0), providing a measure of changes in BLT spatial extent relative to CTRL. When precipitation is suppressed (SENS1), the BLT decreases substantially across all seasons, particularly during Fall, where the BLT extent reduces by 47% (refer to Table 1). It almost diminishes in the AS and gets reduced by ~10-15m in the BoB. In the absence of river runoff (SENS2), the reduction in BLT is comparatively modest (less than 3% in most seasons), with localized shallowing along the eastern coast of India where the influence of the Ganga-Brahmaputra plume is most pronounced. The combined removal of precipitation and runoff (SENS3) further accentuates the reduction in BLT, with changes of similar magnitude to SENS1 but slightly more pronounced in AS and BoB (with some regions being BLT-free). It is noted that the western coast of India is completely BLT-free during the Fall season in the SENS1 and SENS3 experiments. Reducing freshwater input decreases freshwater-driven buoyancy input, weakening the haline stratification.

Conversely, when freshwater input is increased (SENS4), precipitation and river discharge increase the BLT across all seasons. The increase is strongest during the summer (10%) and fall (8%), coinciding with peak monsoonal precipitation and river discharge, respectively. The freshening leads to a further spatially expansive BLT and makes it deeper. We observe a deepening of the BLT in areas where it typically remains shallow (e.g., NEAS). These results support the view that riverine effects are spatially confined and primarily influence nearshore stratification (e.g., NWBoB), whereas precipitation governs the basin-scale BLT footprint and large-scale salinity gradients (Akhil et al., 2014; de Boyer et al., 2007; Vinayachandran et al., 2002).

3.3 N^2 variability response to freshwater forcing

https://doi.org/10.5194/egusphere-2026-3223
Preprint. Discussion started: 6 July 2026

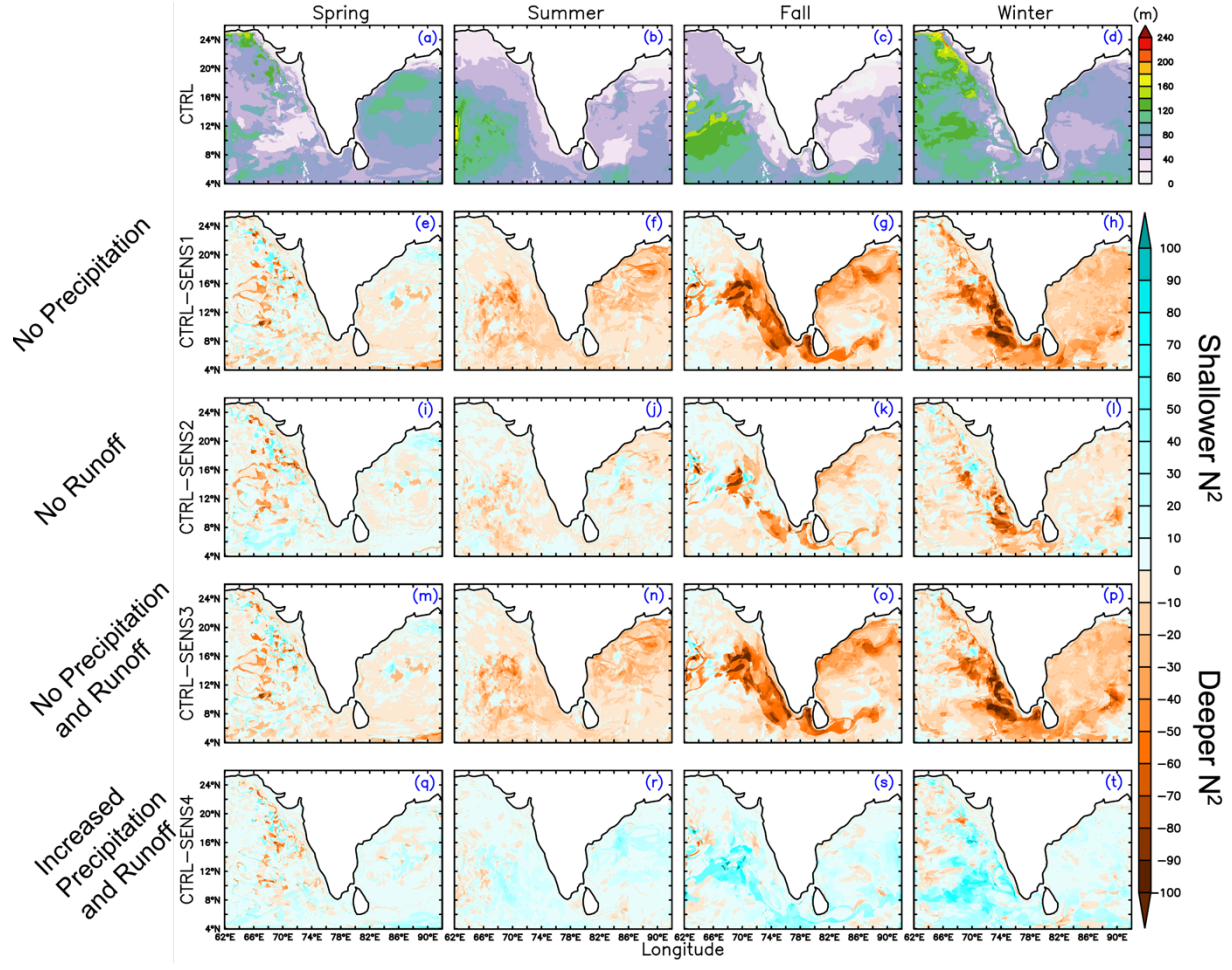

Figure 3. (a-d) Seasonal depth of the maximum N^2 (Brunt-Vaisala frequency) for the CTRL experiment (in meters). (e-t) Difference in the depth of maximum N^2 between the CTRL and SENS experiments. Orange indicates a deepening of the N^2 maximum, whereas blue indicates shoaling, relative to CTRL.

As density in the model is derived from temperature and salinity, variations in freshwater input primarily influence N^2 through changes in haline stratification. In the SENS experiments, the depth of maximum N^2 exhibits a distinct spatial and basin-wide response pattern (Fig. 3). In the CTRL run, the depth of maximum N^2 is shallowest along the NWBoB, particularly in the eastern coastal regions, and deepest in the NAS during the winter and fall seasons (Fig. 3a-d). This suggests that in CTRL, haline stratification places the strongest density gradients nearer the surface in the BoB, especially during the wet seasons. In SENS1, the maximum N^2 depth deepens sharply (orange shading), particularly during the fall and winter. The loss of precipitation reduces the freshwater input and weakens near-surface haline stratification, allowing stronger mixing and a deeper density gradient maximum. SENS2 shows a weaker deepening compared to SENS1 and SENS3. In SENS3, the depth of maximum N^2 is very similar to that in SENS1. In these freshwater-reduced experiments, the

https://doi.org/10.5194/egusphere-2026-3223
Preprint. Discussion started: 6 July 2026

deepening of the N^2 maximum is particularly notable along the Indian coast, especially in the NEAS and SEAS regions. In contrast, the deepening of the N^2 maximum is smaller in magnitude in the BoB, although Its spatial extent is broader.

On the contrary, in SENS4, the pattern reverses: the depth of maximum N^2 shoals (blue shading) in both the AS and the BoB across all seasons, but particularly in the fall and winter. Interestingly, regions that previously showed the most pronounced deepening of N^2 maxima in SENS1-3 (e.g., SEAS) show the strongest shoaling in SENS4, which can be linked to increased localized precipitation and coastal runoff. SENS4 increases near-surface haline stratification due to greater freshwater input, resulting in stronger buoyancy stability and a shallower depth of maximum N^2. This intensified haline stratification under enhanced freshwater input suppresses vertical exchange by strengthening buoyancy stability, consistent with earlier findings (Akhil et al., 2014; Rao and Sivakumar, 2003; Vinayachandran et al., 2002).

3.4 Seasonal and coastal variability in N^2 profiles

The seasonal vertical profiles of N^2 averaged over the five coastal masks show distinct regional patterns in buoyancy stratification across the sensitivity experiments (supporting information Fig. S6). In the NAS, the N^2 maxima occur at greater depths during fall and winter, consistent with the strong vertical mixing typical of this region (Kumar and Prasad, 1996; Kumar et al., 2001). In contrast, spring and summer profiles remain weakly stratified, and all SENS experiments closely overlap with the CTRL run, indicating that freshwater perturbations exert minimal influence on local stratification (Behara and Vinayachandran, 2016; de Boyer et al., 2007). The NEAS displays a similar vertical structure, although the N^2 maxima are slightly shallower compared to NAS. The profiles from all experiments remain nearly coincident during spring and summer, suggesting little variability among the runs. A slight deviation between SENS4 and the other runs in winter suggests a modest increase in near-surface stability due to excess freshwater, consistent with occasional transient freshwater plumes and surface stratification observed in this region during the late monsoon (Shankar et al., 2015). In the SEAS, the contrasts among experiments are more evident. During fall and winter, the N^2 maxima in SENS1 and SENS3 exist at deeper depths than in CTRL, while SENS4 exhibits a pronounced shoaling of the N^2 maxima (Thadathil et al., 2008; Vinayachandran et al., 2002). These variations highlight the stronger seasonal response of SEAS to freshwater changes, particularly under varying precipitation and runoff scenarios.

The SWBoB shows moderate deviations between the runs, most apparent during fall and winter. The depth of maximum N^2 varies slightly, with SENS4 being consistently shallower and SENS1 or SENS3 slightly deeper than CTRL, reflecting a weaker but noticeable sensitivity to freshwater forcing (Akhil et al., 2014; Sherin et al., 2023). In the NWBoB, the vertical profiles show the most pronounced seasonal variability. During summer and fall, corresponding to the peak monsoon and river runoff periods, N^2 maxima deepen in SENS1 and SENS3, while SENS4 displays a distinct shoaling. This contrast indicates a strong dependence of vertical stability on freshwater input in this region (Jarugula et al., 2024; Rao and Sivakumar, 2003). Except in the NAS, all other coastal masks show a consistent pattern: SENS1 and SENS3 depict a deeper

https://doi.org/10.5194/egusphere-2026-3223
Preprint. Discussion started: 6 July 2026

N^2 maxima, whereas SENS4 produces a shallower stratification. During spring, when freshwater input is minimal, the profiles from all runs converge, representing the background thermohaline structure rather than freshwater-induced stratification differences (de Boyer et al., 2007; Vinayachandran et al., 2002).

3.5 Inter-to-intra-seasonal variability of NPP under different freshwater forcing scenarios

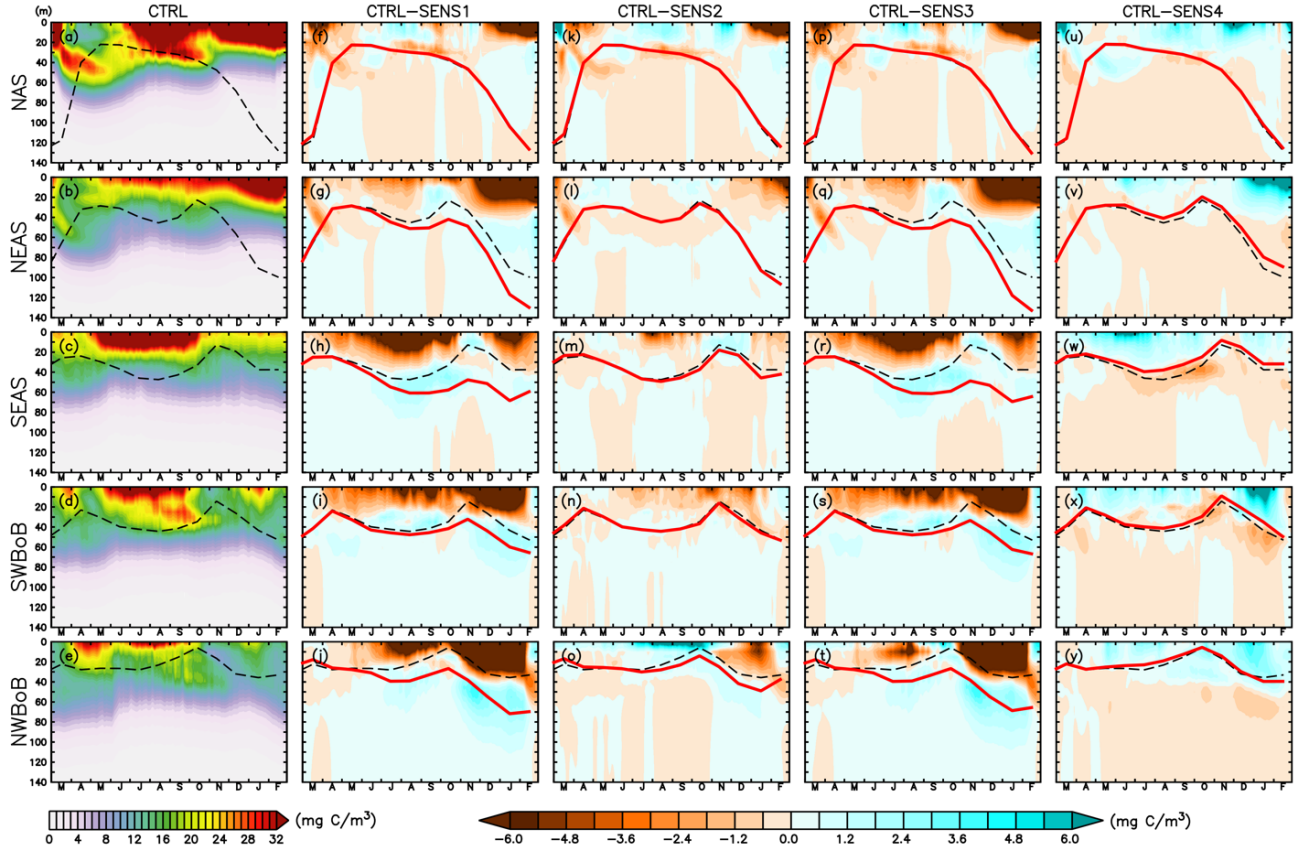

Figure 4. Monthly variability of subsurface NPP (mg C m^{-3}) in the upper 140 m averaged across the five coastal masks. The first column shows the CTRL NPP, while subsequent columns represent CTRL-SENS differences. Brown shading indicates increased NPP in the SENS runs relative to CTRL, whereas blue shading indicates a reduction. The dashed black line denotes the CTRL MLD, and solid red lines indicate MLD in the SENS experiments.

NPP exhibits a gradual decrease in productivity from west to east across the Indian coastal waters, with the NAS being the most productive and the NWBoB the least productive (Kumar et al., 2000, 2002). Productivity remains confined to ~70 m during spring and shoals during late winter. In SENS1, NPP increases slightly in the upper 20 m during winter, accompanied by a deeper MLD. However, a slight decrease in NPP is observed around 20 m, particularly during July-August and November, when the MLD is shallow. SENS2 and SENS3 exhibit a similar pattern. In contrast, NPP in the upper water

https://doi.org/10.5194/egusphere-2026-3223
Preprint. Discussion started: 6 July 2026

column decreases throughout the season in SENS4 due to enhanced stratification. It is noteworthy that freshwater perturbations have little influence on the NAS MLD, as indicated by the nearly coincident MLD profiles across all experiments. Nevertheless, modest changes in NPP are still evident.

The NEAS CTRL run shows persistent near-surface productivity, with a moderate increase during winter. Productivity weakens in spring as stratification increases. Both SENS1 and SENS3 show increased NPP during winter and early spring. It should be noted that this region becomes BLT-free in experiments SENS1 and SENS3 (refer to Sect. 3.2), as also indicated by the increase in MLD, which depicts stronger mixing. The effect in SENS2 is less pronounced, with a marginal increase in NPP within the upper waters. SENS4 exhibits a clear suppression of NPP in winter, as the MLD remains shallower than in CTRL due to enhanced stratification. The SEAS CTRL run shows the highest NPP during the summer, due to strong coastal upwelling (Gupta et al., 2016). It has relatively lower productivity than the NAS and NEAS, which receive a consistent influx of nutrients through either upwelling along the coasts of Oman and Somalia or via convective mixing. SENS1 and SENS3 depict increased NPP, particularly during summer and winter, when the effect of the freshwater-induced BLT is absent. This is further supported by the deepening of the MLD by ~20-40 m relative to CTRL. SENS2 shows a marginal increase in NPP, as this region is not influenced by major river inflows. Conversely, SENS4 consistently suppresses productivity, particularly in the upper 50 m, with the MLD remaining persistently shallower than in CTRL throughout the seasons.

The SWBoB and NWBoB regions exhibit lower NPP than the AS (Kumar et al., 2002), with weaker seasonality and shallower subsurface maxima. However, these regions show the highest and most consistent increase in NPP in SENS1 and SENS3, as they are strongly influenced by precipitation- and river runoff-induced freshwater input. The most pronounced increase in NPP occurs during the fall and early winter seasons, when the freshwater-induced BLT is reduced, leading to deeper mixing. SENS4 shows widespread suppression (a bias of 1-4 mg C m^{-3}) across all seasons, especially in the upper 40 m, where the MLD remains shallower. It is to be noted that in the freshwater-reduced experiments, except for the NAS, regions that show an increase in NPP in the upper waters also exhibit a marginal reduction in subsurface NPP. In contrast, SENS4 (freshwater-enhanced) shows the opposite pattern, with lower surface NPP but a marked increase in subsurface NPP across all regions. This shows how perturbation in freshwater can redistribute nutrients and influence mixing, thereby impacting NPP (particularly regenerative production). The similarity between SENS1 and SENS3 indicates that precipitation exerts a stronger control on NPP variability than river runoff alone.

https://doi.org/10.5194/egusphere-2026-3223
Preprint. Discussion started: 6 July 2026

3.6 Inter-to-intra-seasonal variability of pH under different freshwater forcing scenarios

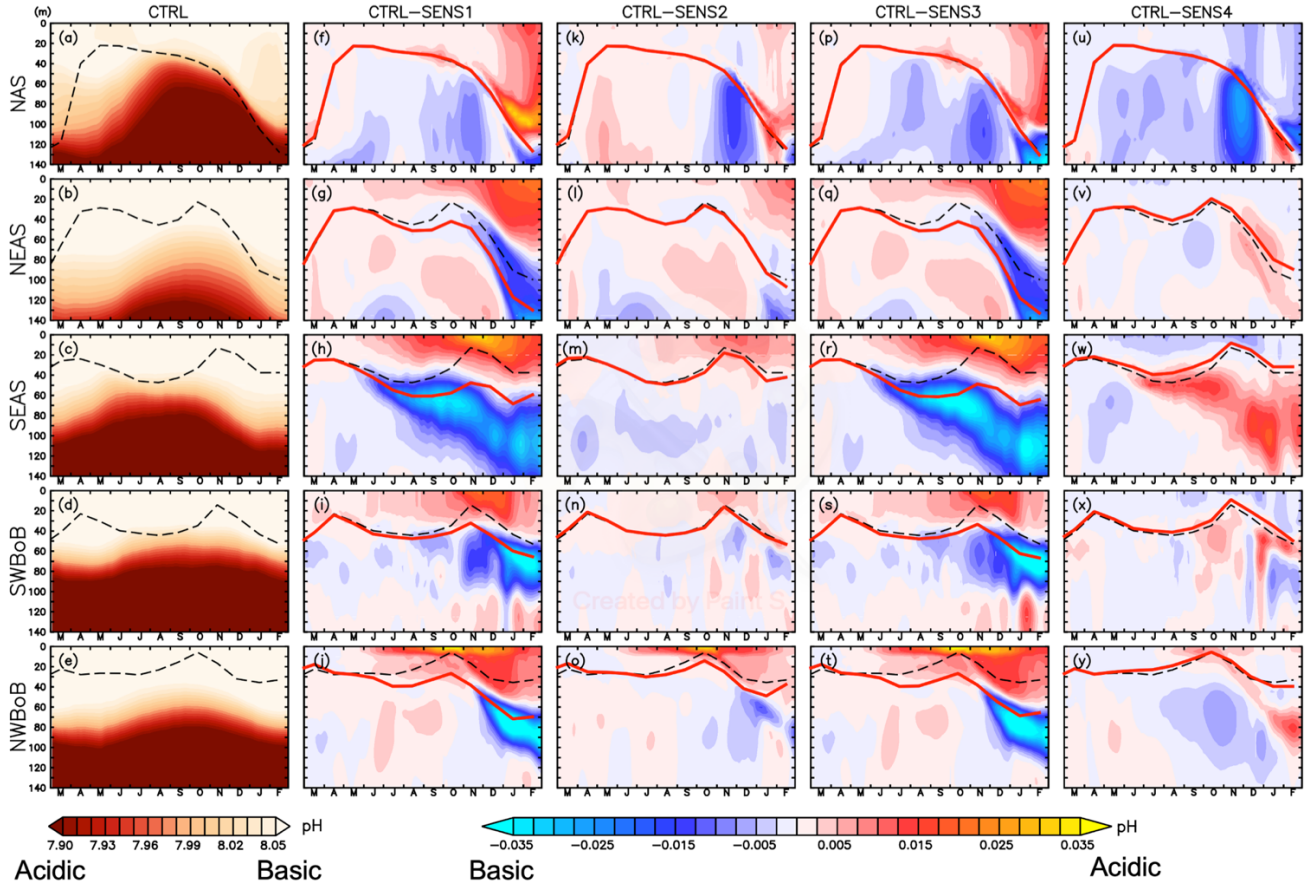

340 **Figure 5. Monthly variability of subsurface pH (non-dimensional) in the upper 140 m averaged across the five coastal masks. The first column (a-e) shows CTRL pH, while the subsequent columns (f-y) represent CTRL-SENS differences. Blue shading indicates a higher pH (i.e., less acidic) in the SENS runs relative to CTRL, whereas red shading indicates a lower pH. The dashed black line denotes the CTRL MLD, and the solid red line indicates MLD in the SENS experiments.**

345 The pH distribution in the upper water column reveals a distinct west-east gradient across the Indian coastal waters, with the AS generally exhibiting lower pH than the BoB. Our findings align with existing studies reporting the prevalence of upwelled, carbon-rich waters in the AS (Madkaiker et al., 2023; Sreeush et al., 2019). Across all regions, the vertical pH structure shows higher near-surface pH during stratified periods and lower pH during intense mixing events, particularly during the winter and summer monsoon seasons.

https://doi.org/10.5194/egusphere-2026-3223
Preprint. Discussion started: 6 July 2026

In the CTRL run for the NAS, the surface shows a marginally higher pH in spring and a lower pH in winter. The subsurface pH gradient shoals toward the surface from summer to early winter due to intense mixing, as reflected in the deepening MLD during this period. SENS1-SENS3 indicates lower pH values (0.01 to 0.025) in the upper waters, particularly during winter, notably above the MLD. However, when convective mixing begins, higher pH values occur below the MLD, particularly during late fall and early winter. In SENS4, we observe higher pH throughout the entire water column up to 140 m. Overall, pH variability in the NAS exhibits a weaker sensitivity to freshwater perturbations than in the other regions.

The NEAS exhibits behaviour similar to that of NAS, but with slightly weaker magnitudes. In the CTRL run, surface pH remains relatively low due to weak coastal upwelling along the Indian coast and the offshore advection of carbon-rich waters from the Oman coast. In SENS1 and SENS3, a deeper winter MLD leads to lower pH within the upper 60 m and higher pH below this depth, particularly during winter. SENS2 shows smaller anomalies, suggesting that the absence of river runoff alone has a limited impact. In contrast, SENS4 shows marginally higher surface pH (up to 0.005) and lower subsurface pH, driven by freshwater-enhanced stratification that inhibits carbon exchange. In the SEAS, CTRL pH shows strong seasonal modulation linked to intense coastal upwelling during summer. In SENS1 and SENS3, BLT suppression leads to stronger vertical mixing, resulting in lower pH above 40 m and higher pH below 60 m from summer to winter. This contrast is clearly separated by the MLD. The magnitude of pH variability is the strongest here among all regions. SENS2 shows a weak pattern of low surface pH, whereas SENS4 shows the opposite structure, with higher surface pH and lower subsurface pH due to enhanced stratification that restricts carbon flux upward.

In the SWBoB, CTRL surface pH values are higher (~8.00-8.03) than in the AS, with marginal shoaling of pH gradients during summer due to weaker coastal upwelling. SENS1-3 shows a clear surface pH reduction (by 0.015-0.02), with peak reduction during November-December, aligned with deeper MLDs and enhanced mixing. Below 80 m, pH becomes higher. In SENS4, the pattern reverses, showing higher pH in the upper 30 m and lower pH below. The surface NWBoB is characterized by high pH values (~8.02-8.05) and weak seasonality in CTRL. The SENS1-3 experiments show notable surface pH reductions (up to 0.03), with peak reductions during October-November, about one month earlier than in the SWBoB, coinciding with a deepening MLD and reduced BLT. Below the MLD, pH is higher (~0.035), confirming enhanced upward mixing of subsurface carbon. SENS4 again shows the opposite behaviour, consistent with freshwater-strengthened stratification.

Overall, the freshwater-reduced experiments exhibit a consistent two-layered pH response: lower pH above the MLD and higher pH below, whereas the freshwater-enhanced scenario shows the reverse. This behaviour highlights the coupling between freshwater forcing, vertical mixing, and carbon redistribution along the Indian coastal waters, consistent with observed regional contrasts between the AS and BoB (Chakraborty et al., 2021; Madkaiker et al., 2023; Resplandy et al., 2012; Sarma et al., 2018). A similar inter-to-intra-seasonal variability analysis of density has been conducted and detailed in the supporting information (Text S2 and Fig. S7).

https://doi.org/10.5194/egusphere-2026-3223
Preprint. Discussion started: 6 July 2026

3.7 Seasonal variability of phytoplankton vertical structure under different freshwater forcing scenarios

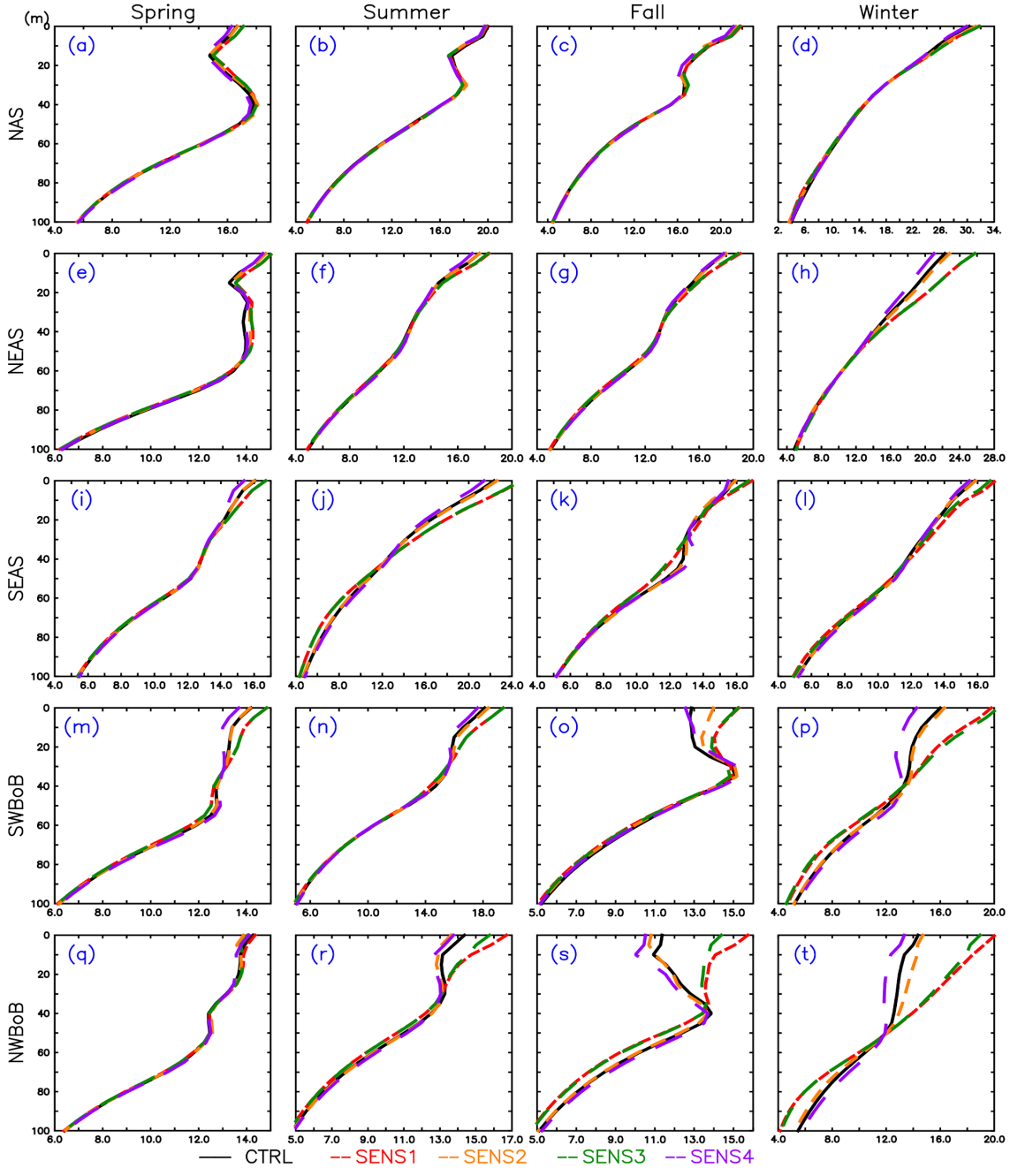

Figure 6. Seasonal mean vertical profiles of small (coccolithophores) phytoplankton biomass expressed as carbon concentration (mmol C m^{-3}) averaged over different seasons in the upper 100 m for the five coastal regions. The black, red, orange, green, and purple lines represent CTRL, SENS1, SENS2, SENS3, and SENS4, respectively.

https://doi.org/10.5194/egusphere-2026-3223
Preprint. Discussion started: 6 July 2026

The vertical profiles of small phytoplankton biomass (SP; Fig. 6) depict distinct regional and seasonal contrasts between the AS and BoB. The AS regions (NAS, NEAS, SEAS) are overall more productive than the BoB, consistent with the stronger vertical nutrient influx and episodic upwelling events that sustain surface chlorophyll concentrations (Gauns et al., 2005; Prasanna Kumar et al., 2002; Vinayachandran et al., 2021). Among these, the NAS exhibits the highest SP values, peaking during winter, while the NEAS and SEAS show moderate enhancement in summer linked to monsoon-driven upwelling. The vertical gradients in SP are generally weak, with biomass concentrated near the surface, particularly in summer and fall when stratification confines growth to the euphotic zone. In SENS1 and SENS3, SP increases by approximately 10-20 % relative to CTRL, particularly in the NEAS during winter and SEAS during summer, whereas SENS4 shows a marginal decrease due to freshwater-enhanced stratification suppressing vertical nutrient exchange. In the BoB (SWBoB and NWBoB), SP maxima occur in the subsurface (~30-60 m), especially during fall, with the strongest variability in fall-winter when stratification weakens. In contrast, SENS4 exhibits a weaker vertical SP profile, suggesting reduced vertical mixing or more persistent stratification, thereby reducing nutrient flux into the euphotic zone (Sarma, 2022).

https://doi.org/10.5194/egusphere-2026-3223
Preprint. Discussion started: 6 July 2026

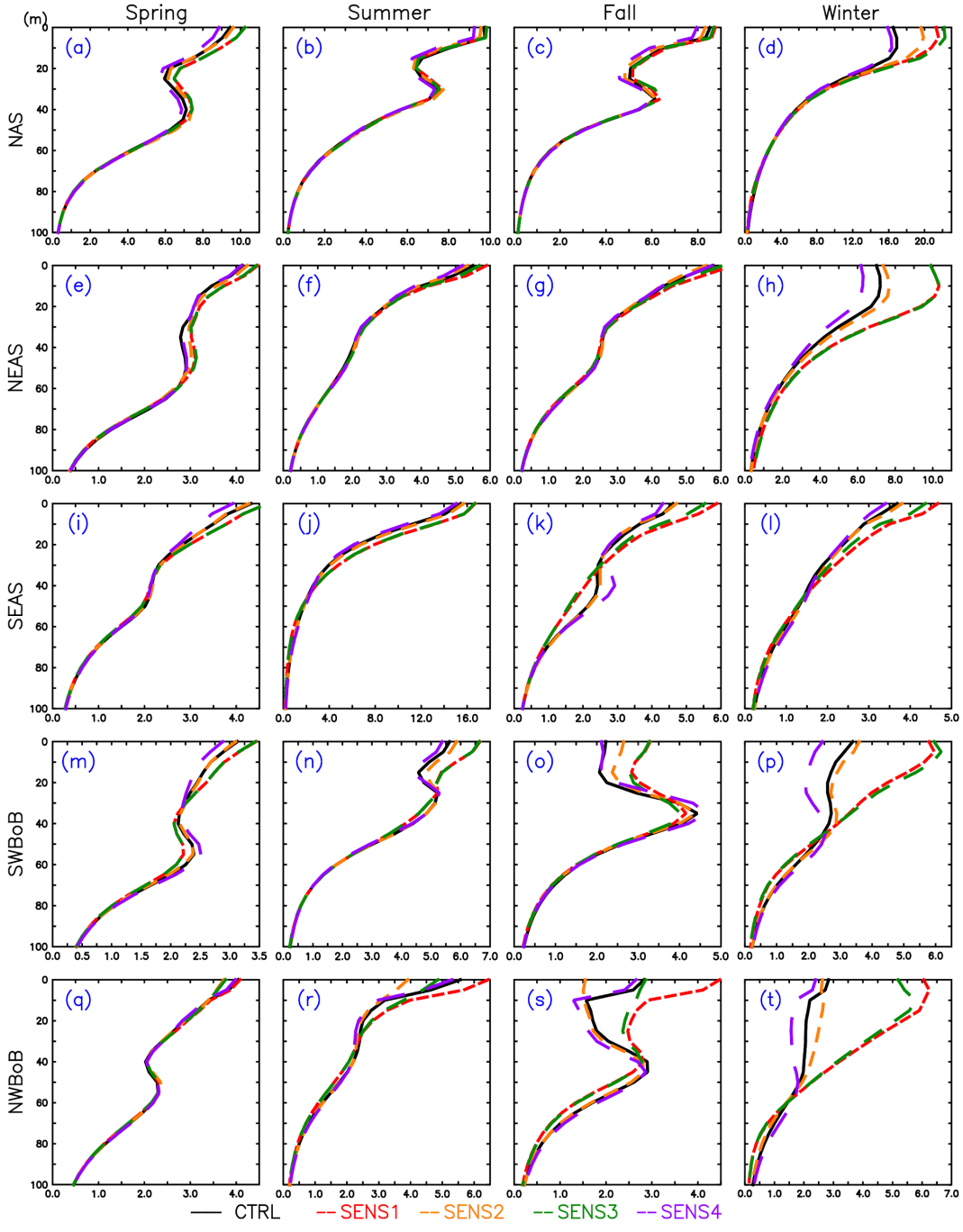

400 **Figure 7. Seasonal mean vertical profiles of large (diatoms) phytoplankton biomass expressed as carbon concentration (mmol C m^{-3}) averaged over different seasons in the upper 100 m for the five coastal regions. The black, red, orange, green, and purple lines represent CTRL, SENS1, SENS2, SENS3, and SENS4, respectively.**

https://doi.org/10.5194/egusphere-2026-3223
Preprint. Discussion started: 6 July 2026

The large phytoplankton biomass (LP; Fig. 7) exhibits stronger vertical gradients and higher sensitivity to freshwater perturbations than SP. Seasonal variability is most pronounced in winter across all regions, consistent with deeper mixing and higher nutrient resupply (Narvekar and Kumar, 2014). In the AS, LP maxima occur near the surface during winter, with secondary peaks between 30-60m in other seasons. SENS1 and SENS3 display up to 15-25% enhancement in LP during winter in the NAS and NEAS, coinciding with increased vertical entrainment of nutrients, whereas SENS4 shows a marginal reduction compared to CTRL. The SEAS region shows a distinct summer maximum, consistent with intense upwelling along the eastern coast of India. In contrast, the BoB regions (SWBoB, NWBoB) exhibit subsurface LP maxima during fall, like SP, but with stronger vertical gradients and variability confined to fall and winter. The magnitude of LP reduction under SENS4 is the highest here, highlighting the strong control of freshwater stratification. The overall order of biomass across experiments is SENS3 ≈ SENS1 > SENS2 > CTRL > SENS4, highlighting that freshwater perturbations govern nutrient accessibility, thereby shaping the vertical structure of phytoplankton functional groups in coastal waters of India. Across most regions and seasons, SP follows a similar ordering, with biomass highest in SENS1 and SENS3 and lowest in SENS4. The larger response of LP relative to SP suggests that freshwater-driven changes in BLT and vertical mixing preferentially affect nutrient-demanding phytoplankton groups. In regions where BLT weakens and nutrient entrainment increases, LP exhibits a much stronger biomass response than SP, indicating a potential shift in phytoplankton community structure under changing freshwater regimes (Henson et al., 2021; Marañón, 2015).

4 Discussions

This study reports that the factor linking freshwater forcing and coastal biogeochemistry is the formation and change in BLT. The presence of BLT reduces vertical mixing between the MLD and the subsurface, thereby limiting the upward movement of nutrient- and carbon-rich waters (de Boyer et al., 2007; Vinayachandran et al., 2002). Therefore, changes in freshwater flux modify BLT, which then affects vertical mixing, N^2, and pycnocline depth. These physical processes directly control nutrient availability, primary productivity, and carbonate chemistry. Under reduced freshwater forcing (SENS1-SENS3), the BLT weakens or disappears in many of the coastal regions. The weaker BLT allows stronger vertical mixing, deepening the MLD and the N^2 maximum, thereby enhancing upward transport of subsurface carbon and nutrients. As a result, surface nutrient supply and NPP increase, especially in regions where haline stratification has been the main factor suppressing mixing, such as the SWBoB, NWBoB, and parts of SEAS. The close similarity between SENS1 and SENS3 indicates that precipitation exerts a stronger control on upper-ocean stratification and biogeochemical variability than river runoff alone across most coastal regions.

In contrast, excess freshwater forcing (SENS4) strengthens and thickens the BLT. A thicker BLT shoals the pycnocline, reduces vertical exchange, and limits nutrient entrainment, resulting in lower NPP and a shallower MLD. The surface water becomes more buoyant and less ventilated, which restricts production, particularly the regenerative component, even when other conditions, such as light, are favourable (Lévy et al., 2007; Kumar et al., 2002).

https://doi.org/10.5194/egusphere-2026-3223
Preprint. Discussion started: 6 July 2026

These physical changes also influence carbonate chemistry. When mixing intensifies (SENS1-SENS3), carbon-rich subsurface waters are entrained to the surface, leading to lower surface pH (more acidic conditions). At the same time, the subsurface becomes relatively less acidic as some carbon is transported upward. Conversely, stronger stratification (SENS4) keeps carbon below shallow MLD, resulting in higher surface pH (less acidic) and lower subsurface pH. This opposite surface-subsurface pH pattern arises from carbon redistribution and agrees with earlier findings (Resplandy et al., 2012; Sarma et al., 2018). Therefore, freshwater-driven BLT changes strongly influence both productivity and surface acidification. Regionally, the results explain why BoB is more sensitive to freshwater changes than AS. The BoB receives large river discharge and heavy monsoonal precipitation, which create strong haline stratification and thick BLT. Hence, small changes in freshwater flux can lead to large changes in BLT and stratification, thereby affecting its biogeochemical state (Akhil et al., 2014; Rao and Sivakumar, 2003).

In contrast, the AS is mainly influenced by evaporation, wind, and upwelling, where mechanical mixing dominates (Madhupratap et al., 1996; Kumar et al., 2001). However, our study shows that coastal runoff, particularly along the western coast of India, plays an important role in modulating upper ocean mixing and biogeochemistry, as demonstrated by the SENS experiments. An exception is the NAS, where freshwater perturbations produce relatively small changes in MLD, yet modest changes in NPP and pH remain evident. Additional factors, such as nutrient entrainment across the base of the mixed layer and lateral transport processes, may also contribute to these responses (Kumar et al., 2000, 2001; Wiggert et al., 2006).

A few key results and implications can be summarized as follows:

(a) Reduced freshwater input may increase productivity, especially in the BoB, due to weakened BLT, stronger mixing, and enhanced nutrient entrainment.
(b) Reduced freshwater also leads to lower surface pH because carbon-rich subsurface water reaches the surface during the same mixing events that support productivity. This indicates a trade-off between higher productivity and increased surface acidification.
(c) Increased freshwater strengthens the BLT, reducing mixing and nutrient supply and leading to lower productivity, as shown in SENS4 over the BoB and parts of the SEAS.
(d) Reduced freshwater also deepens the stratification and slightly weakens it, especially during fall and winter. Interestingly, the deepening is more pronounced in the SEAS than in the BoB, contrasting with conventional wisdom. This result suggests that coastal freshwater inputs along the western coast of India can exert a stronger control on upper-ocean stratification than is commonly assumed, despite the much larger freshwater inventory of the BoB. This distinction requires further investigation.

Finally, accurate representation of precipitation and river runoff is critical because their spatial and seasonal variations control the freshwater balance and its biogeochemical impacts (Boulange et al., 2021; Pokhrel et al., 2018; Savelli et al.,

https://doi.org/10.5194/egusphere-2026-3223
Preprint. Discussion started: 6 July 2026

2026). Second, the opposing effects on productivity and surface pH indicate that freshwater-driven changes can elicit complex ecosystem responses. These contrasting responses demonstrate that enhanced biological productivity does not necessarily imply improved carbonate-system conditions. Therefore, both productivity and ocean acidification need to be considered together when assessing the impacts of freshwater variability on coastal marine ecosystems. For this, a holistic understanding of biogeochemical and ecological modelling is required to assess the overall ecosystem impacts, which must be carefully examined.

5 Conclusions

This study examined the role of freshwater forcing in shaping the physical and biogeochemical state of the coastal waters adjoining the Indian subcontinent using a set of sensitivity experiments. Our analysis shows that the spatial and temporal variability of freshwater fluxes strongly influences stratification, BLT, and nutrient entrainment, thereby affecting the regional patterns of surface productivity and ocean acidification.

Under reduced freshwater input, the BLT weakens, and vertical mixing intensifies, allowing higher nutrient entrainment into the euphotic zone. This effect is particularly evident over the BoB, where stratification is generally strong and subsurface nutrient availability remains limited. As a result, this supports higher primary productivity, reflecting a more efficient upward transport of nutrients to the surface. However, the same mixing events also bring carbon-rich subsurface waters to the surface, leading to a noticeable decline in surface pH. This reveals a clear trade-off between enhanced productivity and increased acidification, indicating that stronger vertical exchange, while beneficial for nutrient supply, can intensify acidification stress at the surface.

In contrast, increased freshwater input strengthens the BLT and enhances near-surface stratification, suppressing vertical mixing and limiting nutrient supply to the euphotic zone. This reduction in nutrient availability results in weaker productivity, particularly across the BoB and parts of the SEAS. These results collectively emphasize that freshwater-induced stratification is a key regulator of both the magnitude and spatial extent of biological productivity in the region of analysis. The reduced freshwater experiments also deepen the depth N^2 maximum, which is more pronounced in the SEAS than in the BoB. This result suggests that coastal freshwater inputs along the western coast of India can exert a stronger control on upper-ocean stratification than is commonly assumed, despite the much larger freshwater inventory of the BoB. The mechanisms responsible for this behaviour require further investigation. Understanding these processes is essential to interpreting how freshwater variability controls the vertical structure and nutrient pathways.

Overall, reduced freshwater promotes productivity at the expense of higher surface acidification, while increased freshwater suppresses productivity but maintains surface pH through stronger stratification. These opposing effects highlight the

https://doi.org/10.5194/egusphere-2026-3223
Preprint. Discussion started: 6 July 2026

complex interactions between freshwater forcing, biological productivity, and carbonate chemistry under varying freshwater regimes.

The larger response of LP relative to SP suggests that freshwater-driven changes in BLT and vertical mixing preferentially affect nutrient-demanding phytoplankton groups. In regions where BLT weakens and nutrient entrainment increases, LP exhibits a much stronger biomass response than SP, indicating a potential shift in phytoplankton community structure under changing freshwater regimes. In a warming climate, where monsoon intensity, river discharge, and glacial melt are projected to shift, the feedback among freshwater forcing, biogeochemical cycling, and acidification requires continued and more detailed investigation.

Code availability

The MITgcm model code can be freely downloaded from the Zenodo open data repository (https://doi.org/10.5281/zenodo.18371317, Campin et al., 2026).

Data availability

MUR SST was downloaded from https://podaac.jpl.nasa.gov/dataset/MUR-JPL-L4-GLOB-v4.1 (Chin et al., 2017). SMAP SSS was downloaded from https://podaac.jpl.nasa.gov/dataset/SMAP_JPL_L3_SSS_CAP_MONTHLY_V5 (Tang et al., 2017). SMOS SSS was downloaded from https://doi.org/10.17882/52804 (Boutin et al., 2023). CORA data were downloaded from https://doi.org/10.17882/46219 (Szekely et al., 2024). The DIC climatology data used for model forcing are available at https://digital.csic.es/handle/10261/200537 (Broullon et al., 2020). The ALK and nutrient climatology can be downloaded from https://digital.csic.es/handle/10261/184460 (Broullon et al., 2019). Dissolved iron data is available at https://data.marine.copernicus.eu/product/GLOBAL_MULTIYEAR_BGC_001_029/. Atmospheric pCO_2 can be downloaded from https://gml.noaa.gov/ccgg/mbl/data.php (Andrews et al., 2014). MATLAB and PyFerret software were used for analysis and data visualization.

Author contributions

Conceptualization: KM, ADR; methodology: KM; software: KM, JML; validation: KM; formal analysis: KM; investigation: KM, ADR and JML; resources: ADR, VP; writing (original draft preparation): KM; writing (review and editing): KM, ADR, VP and JML; visualization: KM; supervision: ADR, VP. All authors have read and approved the version of the manuscript.

https://doi.org/10.5194/egusphere-2026-3223
Preprint. Discussion started: 6 July 2026

Competing interests

The authors declare that they have no conflict of interest.

Acknowledgements

Kunal Madkaiker acknowledges IIT Delhi for the PhD fellowship support and the computational resources provided through its high-performance computing cluster.

Financial support

The authors declare that no funds, grants, or other support were received during the preparation of this manuscript.

References

Acharyya, T., Sarma, V. V. S. S., Sridevi, B., Venkataramana, V., Bharathi, M. D., Naidu, S. A., Kumar, B. S. K., Prasad, V. R., Bandyopadhyay, D., Reddy, N. P. C., and Kumar, M. D.: Reduced river discharge intensifies phytoplankton bloom in Godavari estuary, India, Mar. Chem., 132–133, https://doi.org/10.1016/j.marchem.2012.01.005, 2012.

Akhil, V. P., Durand, F., Lengaigne, M., Vialard, J., Keerthi, M. G., Gopalakrishna, V. V., Deltel, C., Papa, F., and De Boyer Montégut, C.: A modeling study of the processes of surface salinity seasonal cycle in the Bay of Bengal, J. Geophys. Res. Oceans, 119, 3926–3947, https://doi.org/10.1002/2013JC009632, 2014.

Akhil, V. P., Vialard, J., Lengaigne, M., Keerthi, M. G., Boutin, J., Vergely, J. L., and Papa, F.: Bay of Bengal Sea surface salinity variability using a decade of improved SMOS re-processing, Remote Sens. Environ., 248, https://doi.org/10.1016/j.rse.2020.111964, 2020.

Andrews, A. E., Kofler, J. D., Trudeau, M. E., Williams, J. C., Neff, D. H., Masarie, K. A., Chao, D. Y., Kitzis, D. R., Novelli, P. C., Zhao, C. L., Dlugokencky, E. J., Lang, P. M., Crotwell, M. J., Fischer, M. L., Parker, M. J., Lee, J. T., Baumann, D. D., Desai, A. R., Stanier, C. O., De Wekker, S. F. J., Wolfe, D. E., Munger, J. W., and Tans, P. P.: CO2, CO, and CH4 measurements from tall towers in the NOAA earth system research laboratory's global greenhouse gas reference network: Instrumentation, uncertainty analysis, and recommendations for future high-accuracy greenhouse gas monitoring efforts, Atmos. Meas. Tech., 7, 647–687, https://doi.org/10.5194/AMT-7-647-2014, 2014.

Behara, A. and Vinayachandran, P. N.: An OGCM study of the impact of rain and river water forcing on the Bay of Bengal, J. Geophys. Res. Oceans, 121, https://doi.org/10.1002/2015JC011325, 2016.

Behara, A., Vinayachandran, P. N., and Shankar, D.: Influence of Rainfall Over Eastern Arabian Sea on Its Salinity, J. Geophys. Res. Oceans, 124, https://doi.org/10.1029/2019JC014999, 2019.

https://doi.org/10.5194/egusphere-2026-3223
Preprint. Discussion started: 6 July 2026

Boulange, J., Hanasaki, N., Yamazaki, D., and Pokhrel, Y.: Role of dams in reducing global flood exposure under climate change, Nat. Commun., 12, https://doi.org/10.1038/s41467-020-20704-0, 2021.

Boutin Jacqueline, Vergely Jean-Luc, Khvorostyanov Dmitry, and Supply Alexandre: SMOS SSS L3 maps generated by CATDS CEC LOCEAN. debias V8.0. SEANOE., https://doi.org/https://doi.org/10.17882/52804, 2023.

de Boyer Montégut, C., Mignot, J., Lazar, A., and Cravatte, S.: Control of salinity on the mixed layer depth in the world ocean: 1. General description, J. Geophys. Res. Oceans, 112, https://doi.org/10.1029/2006JC003953, 2007.

Broullón, D., Pérez, F. F., Velo, A., Hoppema, M., Olsen, A., Takahashi, T., Key, R. M., Tanhua, T., González-Dávila, M., Jeansson, E., Kozyr, A., and Van Heuven, S. M. A. C.: A global monthly climatology of total alkalinity: A neural network approach, Earth Syst. Sci. Data, 11, https://doi.org/10.5194/essd-11-1109-2019, 2019.

Broullón, D., Pérez, F. F., Velo, A., Hoppema, M., Olsen, A., Takahashi, T., Key, R. M., Tanhua, T., Magdalena Santana-Casiano, J., and Kozyr, A.: A global monthly climatology of oceanic total dissolved inorganic carbon: A neural network approach, Earth Syst. Sci. Data, 12, https://doi.org/10.5194/essd-12-1725-2020, 2020.

Campin, J.-M., Heimbach, P., Losch, M., Forget, G., edhill3, Adcroft, A., amolod, Menemenlis, D., dfer22, Jahn, O., Hill, C., Scott, J., dngoldberg, stephdut, Mazloff, M., Fox-Kemper, B., antnguyen13, Doddridge, E., Fenty, I., Bates, M., Smith, T., Wang, O., AndrewEichmann-NOAA, mitllheisey, Lauderdale, J., Martin, T., Abernathey, R., samarkhatiwala, Escobar, I., and averdy: MITgcm/MITgcm: checkpoint69k, https://doi.org/10.5281/zenodo.18371317, January 2026.

Chaitanya, A. V. S., Lengaigne, M., Vialard, J., Gopalakrishna, V. V., Durand, F., Kranthikumar, C., Amritash, S., Suneel, V., Papa, F., and Ravichandran, M.: Salinity measurements collected by fishermen reveal a “river in the sea” flowing along the eastern coast of India, Bull. Am. Meteorol. Soc., 95, https://doi.org/10.1175/BAMS-D-12-00243.1, 2014.

Chakraborty, K., Valsala, V., Bhattacharya, T., and Ghosh, J.: Seasonal cycle of surface ocean pCO2 and pH in the northern Indian Ocean and their controlling factors, Prog. Oceanogr., 198, 102683, https://doi.org/10.1016/J.POCEAN.2021.102683, 2021.

Chakraborty, K., Lotliker, A. A., Gupta, G. V. M., Narayanan Nampoothiri S, V., Paul, A., Ghosh, J., Bhattacharya, T., Baliarsingh, S. K., and Samanta, A.: Assessment of an ocean-ecosystem model in simulating the Indian coastal marine ecosystem dynamics, Journal of Operational Oceanography, 15, 137–155, https://doi.org/10.1080/1755876X.2020.1843298;WGROUP:STRING:PUBLICATION, 2022.

Chin, T. M., Vazquez-Cuervo, J., and Armstrong, E. M.: A multi-scale high-resolution analysis of global sea surface temperature, Remote Sens. Environ., 200, https://doi.org/10.1016/j.rse.2017.07.029, 2017.

Dai, A. and Trenberth, K. E.: Estimates of freshwater discharge from continents: Latitudinal and seasonal variations, J. Hydrometeorol., 3, https://doi.org/10.1175/1525-7541(2002)003<0660:EOFDFC>2.0.CO;2, 2002.

Dunne, J. P., Armstrong, R. A., Gnnadesikan, A., and Sarmiento, J. L.: Empirical and mechanistic models for the particle export ratio, Global Biogeochem. Cycles, 19, 4026, https://doi.org/10.1029/2004GB002390, 2005.

Dunne, J. P., Bociu, I., Bronselaer, B., Guo, H., John, J. G., Krasting, J. P., Stock, C. A., Winton, M., and Zadeh, N.: Simple Global Ocean Biogeochemistry With Light, Iron, Nutrients and Gas Version 2 (BLINGv2): Model Description and

https://doi.org/10.5194/egusphere-2026-3223
Preprint. Discussion started: 6 July 2026

Simulation Characteristics in GFDL's CM4.0, J. Adv. Model. Earth Syst., 12, e2019MS002008, https://doi.org/10.1029/2019MS002008, 2020.

Durand, F., Shankar, D., de Boyer Montégut, C., Shenoi, S. S. C., Blanke, B., and Madec, G.: Modeling the barrier-layer formation in the southeastern Arabian Sea, J. Clim., 20, https://doi.org/10.1175/JCLI4112.1, 2007.

Felton, C. S., Subrahmanyam, B., Murty, V. S. N., and Shriver, J. F.: Estimation of the barrier layer thickness in the Indian Ocean using Aquarius Salinity, J. Geophys. Res. Oceans, 119, 4200–4213, https://doi.org/10.1002/2013JC009759;ISSUE:ISSUE:DOI, 2014.

Fournier, S., Vialard, J., Lengaigne, M., Lee, T., Gierach, M. M., and Chaitanya, A. V. S.: Modulation of the Ganges-Brahmaputra River Plume by the Indian Ocean Dipole and Eddies Inferred From Satellite Observations, J. Geophys. Res. Oceans, 122, https://doi.org/10.1002/2017JC013333, 2017.

Galbraith, E. D., Gnanadesikan, A., Dunne, J. P., and Hiscock, M. R.: Regional impacts of iron-light colimitation in a global biogeochemical model, Biogeosciences, 7, 1043–1064, https://doi.org/10.5194/BG-7-1043-2010, 2010.

Gauns, M., Madhupratap, M., Ramaiah, N., Jyothibabu, R., Fernandes, V., Paul, J. T., and Prasanna Kumar, S.: Comparative accounts of biological productivity characteristics and estimates of carbon fluxes in the Arabian Sea and the Bay of Bengal, Deep Sea Research Part II: Topical Studies in Oceanography, 52, 2003–2017, https://doi.org/10.1016/J.DSR2.2005.05.009, 2005.

Goes, J. I., Tian, H., Gomes, H. do R., Anderson, O. R., Al-Hashmi, K., deRada, S., Luo, H., Al-Kharusi, L., Al-Azri, A., and Martinson, D. G.: Ecosystem state change in the Arabian Sea fuelled by the recent loss of snow over the Himalayan-Tibetan Plateau region, Sci. Rep., 10, https://doi.org/10.1038/s41598-020-64360-2, 2020.

Gupta, G. V. M., Sudheesh, V., Sudharma, K. V., Saravanane, N., Dhanya, V., Dhanya, K. R., Lakshmi, G., Sudhakar, M., and Naqvi, S. W. A.: Evolution to decay of upwelling and associated biogeochemistry over the southeastern Arabian Sea shelf, J. Geophys. Res. Biogeosci., 121, 159–175, https://doi.org/10.1002/2015JG003163, 2016.

Hamilton, D. S., Scanza, R. A., Feng, Y., Guinness, J., Kok, J. F., Li, L., Liu, X., Rathod, S. D., Wan, J. S., Wu, M., and Mahowald, N. M.: Improved methodologies for Earth system modelling of atmospheric soluble iron and observation comparisons using the Mechanism of Intermediate complexity for Modelling Iron (MIMI v1.0), Geosci. Model Dev., 12, 3835–3862, https://doi.org/10.5194/GMD-12-3835-2019, 2019.

Henson, S. A., Cael, B. B., Allen, S. R., and Dutkiewicz, S.: Future phytoplankton diversity in a changing climate, Nat. Commun., 12, 1–8, https://doi.org/10.1038/S41467-021-25699-W;SUBJMETA, 2021.

Intergovernmental Panel on Climate Change (IPCC): Climate Change 2022 – Impacts, Adaptation and Vulnerability, Cambridge University Press, https://doi.org/10.1017/9781009325844, 2023.

Jarugula, S., Sengupta, D., Shroyer, E., and Papa, F.: Mixing of Rain and River Water in the Bay of Bengal From Basin-Scale Freshwater Balance, Geophys. Res. Lett., 51, https://doi.org/10.1029/2023GL106451, 2024.

https://doi.org/10.5194/egusphere-2026-3223
Preprint. Discussion started: 6 July 2026

Jayaram, C., Bhaskar, T. V. S. U., Chacko, N., Prakash, S., and Rao, K. H.: Spatio-temporal variability of chlorophyll in the northern Indian Ocean: A biogeochemical argo data perspective, Deep Sea Research Part II: Topical Studies in Oceanography, 183, 104928, https://doi.org/10.1016/J.DSR2.2021.104928, 2021.

Katzenberger, A., Levermann, A., Schewe, J., and Pongratz, J.: Intensification of Very Wet Monsoon Seasons in India Under Global Warming, Geophys. Res. Lett., 49, e2022GL098856, https://doi.org/10.1029/2022GL098856;SUBPAGE:STRING:FULL, 2022.

Kumar, S. P. and Prasad, T. G.: Winter cooling in the northern Arabian Sea, Curr. Sci., 71, 834–841, 1996.

Lévy, M., Shankar, D., André, J. M., Shenoi, S. S. C., Durand, F., and de Boyer Montégut, C.: Basin-wide seasonal evolution of the Indian Ocean's phytoplankton blooms, J. Geophys. Res. Oceans, 112, 12014, https://doi.org/10.1029/2007JC004090, 2007.

Lutz, A. F., Immerzeel, W. W., Shrestha, A. B., and Bierkens, M. F. P.: Consistent increase in High Asia's runoff due to increasing glacier melt and precipitation, Nat. Clim. Chang., 4, 587–592, https://doi.org/10.1038/NCLIMATE2237;TECHMETA, 2014.

Madhupratap, M., Prasanna Kumar, S., Bhattathiri, P. M. A., Dileep Kumar, M., Raghukumar, S., Nair, K. K. C., and Ramaiah, N.: Mechanism of the biological response to winter cooling in the northeastern Arabian Sea, Nature, 384, 549–552, https://doi.org/10.1038/384549A0;KWRD, 1996.

Madkaiker, K., Valsala, V., Sreeush, M. G., Mallissery, A., Chakraborty, K., and Deshpande, A.: Understanding the Seasonality, Trends, and Controlling Factors of Indian Ocean Acidification Over Distinctive Bio-Provinces, J. Geophys. Res. Biogeosci., 128, https://doi.org/10.1029/2022JG006926, 2023.

Madkaiker, K., Rao, A. D., and Joseph, S.: High-resolution numerical modelling of seasonal volume, freshwater, and heat transport along the Indian coast, Ocean Science, 20, 1167–1185, https://doi.org/10.5194/os-20-1167-2024, 2024.

Maharana, P., Dimri, A. P., and Choudhary, A.: Future changes in Indian summer monsoon characteristics under 1.5 and 2 °C specific warming levels, Clim. Dyn., 54, https://doi.org/10.1007/s00382-019-05012-8, 2020.

Marañón, E.: Cell Size as a key determinant of phytoplankton metabolism and community structure, Ann. Rev. Mar. Sci., 7, https://doi.org/10.1146/annurev-marine-010814-015955, 2015.

Marshall, J., Adcroft, A., Hill, C., Perelman, L., and Heisey, C.: A finite-volume, incompressible Navier Stokes model for studies of the ocean on parallel computers, J. Geophys. Res. Oceans, 102, 5753–5766, https://doi.org/10.1029/96JC02775, 1997.

Mazloff, M. R., Heimbach, P., and Wunsch, C.: An eddy-permitting Southern Ocean state estimate, J. Phys. Oceanogr., 40, https://doi.org/10.1175/2009JPO4236.1, 2010.

Naidu, C. V., Durgalakshmi, K., Krishna, K. M., Rao, S. R., Satyanarayana, G. C., Lakshminarayana, P., and Rao, L. M.: Is summer monsoon rainfall decreasing over India in the global warming era?, Journal of Geophysical Research Atmospheres, 114, https://doi.org/10.1029/2008JD011288, 2009.

https://doi.org/10.5194/egusphere-2026-3223
Preprint. Discussion started: 6 July 2026

Naidu, C. V., Dharma Raju, A., Satyanarayana, G. C., Vinay Kumar, P., Chiranjeevi, G., and Suchitra, P.: An observational evidence of decrease in Indian summer monsoon rainfall in the recent three decades of global warming era, Glob. Planet. Change, 127, https://doi.org/10.1016/j.gloplacha.2015.01.010, 2015.

Narvekar, J. and Prasanna Kumar, S.: Mixed layer variability and chlorophyllabiomass in the bay of bengal, Biogeosciences, 11, https://doi.org/10.5194/bg-11-3819-2014, 2014.

Papa, F., Bala, S. K., Pandey, R. K., Durand, F., Gopalakrishna, V. V., Rahman, A., and Rossow, W. B.: Ganga-Brahmaputra river discharge from Jason-2 radar altimetry: An update to the long-term satellite-derived estimates of continental freshwater forcing flux into the Bay of Bengal, J. Geophys. Res. Oceans, 117, https://doi.org/10.1029/2012JC008158, 2012.

Paul, S., Ghosh, S., Oglesby, R., Pathak, A., Chandrasekharan, A., and Ramsankaran, R.: Weakening of Indian Summer Monsoon Rainfall due to Changes in Land Use Land Cover, Sci. Rep., 6, https://doi.org/10.1038/srep32177, 2016.

Pokhrel, Y., Burbano, M., Roush, J., Kang, H., Sridhar, V., and Hyndman, D. W.: A review of the integrated effects of changing climate, land use, and dams on Mekong river hydrology, https://doi.org/10.3390/w10030266, 2018.

Prasanna Kumar, S., Madhupratap, M., Dileep Kumar, M., Gauns, M., Muraleedharan, P. M., Sarma, V. V. S. S., and De Souza, S. N.: Physical control of primary productivity on a seasonal scale in central and eastern Arabian Sea, Proceedings of the Indian Academy of Sciences, Earth and Planetary Sciences, 109, 433–441, https://doi.org/10.1007/BF02708331/METRICS, 2000.

Prasanna Kumar, S., Ramaiah, N., Gauns, M., Sarma, V. V. S. S., Muraleedharan, P. M., Raghukumar, S., Dileep Kumar, M., and Madhupratap, M.: Physical forcing of biological productivity in the Northern Arabian Sea during the Northeast Monsoon, Deep Sea Research Part II: Topical Studies in Oceanography, 48, 1115–1126, https://doi.org/10.1016/S0967-0645(00)00133-8, 2001.

Prasanna Kumar, S., Muraleedharan, P. M., Prasad, T. G., Gauns, M., Ramaiah, N., De Souza, S. N., Sardesai, S., and Madhupratap, M.: Why is the Bay of Bengal less productive during summer monsoon compared to the Arabian Sea?, Geophys. Res. Lett., 29, https://doi.org/10.1029/2002GL016013, 2002.

Rao, R. R. and Sivakumar, R.: Seasonal variability of sea surface salinity and salt budget of the mixed layer of the north Indian Ocean, J. Geophys. Res. Oceans, 108, 9–1, https://doi.org/10.1029/2001JC000907, 2003.

Resplandy, L., Lévy, M., Bopp, L., Echevin, V., Pous, S., Sarma, V. V. S. S., and Kumar, D.: Controlling factors of the oxygen balance in the Arabian Sea's OMZ, Biogeosciences, 9, 5095–5109, https://doi.org/10.5194/BG-9-5095-2012, 2012.

Resplandy, L., Hogikyan, A., Müller, J. D., Najjar, R. G., Bange, H. W., Bianchi, D., Weber, T., Cai, W. J., Doney, S. C., Fennel, K., Gehlen, M., Hauck, J., Lacroix, F., Landschützer, P., Le Quéré, C., Roobaert, A., Schwinger, J., Berthet, S., Bopp, L., Chau, T. T. T., Dai, M., Gruber, N., Ilyina, T., Kock, A., Manizza, M., Lachkar, Z., Laruelle, G. G., Liao, E., Lima, I. D., Nissen, C., Rödenbeck, C., Séférian, R., Toyama, K., Tsujino, H., and Regnier, P.: A Synthesis of Global Coastal Ocean Greenhouse Gas Fluxes, Global Biogeochem. Cycles, 38, e2023GB007803, https://doi.org/10.1029/2023GB007803, 2024.

https://doi.org/10.5194/egusphere-2026-3223
Preprint. Discussion started: 6 July 2026

Sahastrabuddhe, R., Ghausi, S. A., Joseph, J., and Ghosh, S.: Indian Summer Monsoon Rainfall in a changing climate: a review, Journal of Water and Climate Change, 14, https://doi.org/10.2166/wcc.2023.127, 2023.

Sarma, V. V. S. S.: Biogeochemistry of carbon, nitrogen and oxygen in the Bay of Bengal: New insights through re-analysis of data, Journal of Earth System Science, 131, https://doi.org/10.1007/s12040-022-01915-z, 2022.

Sarma, V. V. S. S., Kumari, V. R., Srinivas, T. N. R., Krishna, M. S., Ganapathi, P., and Murty, V. S. N.: East India Coastal Current controls the dissolved inorganic carbon in the coastal Bay of Bengal, Mar. Chem., 205, 37–47, https://doi.org/10.1016/j.marchem.2018.07.010, 2018.

Savelli, R., Carroll, D., Menemenlis, D., Lauderdale, J. M., Bertin, C., Dutkiewicz, S., Manizza, M., Bloom, A. A., Castro-Morales, K., Miller, C. E., Simard, M., Bowman, K. W., and Zhang, H.: Implementing riverine biogeochemical inputs in ECCO-Darwin: a sensitivity analysis of terrestrial fluxes in a data-assimilative global ocean biogeochemistry model, Geosci. Model Dev., 19, 867–885, https://doi.org/10.5194/GMD-19-867-2026, 2026.

Schott, F. A., Xie, S. P., and McCreary, J. P.: Indian ocean circulation and climate variability, Reviews of Geophysics, 47, 1002, https://doi.org/10.1029/2007RG000245;REQUESTEDJOURNAL:JOURNAL:19449208;ISSUE:ISSUE:DOI, 2009.

Sengupta, D., Bharath Raj, G. N., and Shenoi, S. S. C.: Surface freshwater from Bay of Bengal runoff and Indonesian Throughflow in the tropical Indian Ocean, Geophys. Res. Lett., 33, https://doi.org/10.1029/2006GL027573, 2006.

Sengupta, D., Bharath Raj, G. N., Ravichandran, M., Sree Lekha, J., and Papa, F.: Near-surface salinity and stratification in the north Bay of Bengal from moored observations, Geophys. Res. Lett., 43, https://doi.org/10.1002/2016GL068339, 2016.

Shankar, D., Vinayachandran, P. N., and Unnikrishnan, A. S.: The monsoon currents in the north Indian Ocean, https://doi.org/10.1016/S0079-6611(02)00024-1, 2002.

Shankar, D., Remya, R., Vinayachandran, P. N., Chatterjee, A., and Behera, A.: Inhibition of mixed-layer deepening during winter in the northeastern Arabian Sea by the West India Coastal Current, Climate Dynamics 2015 47:3, 47, 1049–1072, https://doi.org/10.1007/S00382-015-2888-3, 2015.

Sherin, V. R., Girishkumar, M. S., Shivaprasad, S., Sureshkumar, N., Farrar, J. T., Athulya, K., Ashin, K., Rama Rao, E. P., Sengupta, D., Venkatesan, R., and Ravichandran, M.: Importance of Seasonally Evolving Near-Surface Salinity Stratification on Mixed Layer Heat Budget During Summer Monsoon Intraseasonal Oscillation in the Northern Bay of Bengal in 2019, J. Geophys. Res. Oceans, 128, https://doi.org/10.1029/2023JC019800, 2023.

Smitha, B. R., Sanjeevan, V. N., Vimalkumar, K. G., and Revichandran, C.: On the upwelling off the southern tip and along the west coast of India, J. Coast. Res., 24, 95–102, https://doi.org/10.2112/06-0779.1/28230/ON-THE-UPWELLING-OFF-THE-SOUTHERN-TIP-AND-ALONG, 2008.

Sprintall, J. and Tomczak, M.: Evidence of the barrier layer in the surface layer of the tropics, J. Geophys. Res. Oceans, 97, https://doi.org/10.1029/92jc00407, 1992.

Sreeush, M. G., Rajendran, S., Valsala, V., Pentakota, S., Prasad, K. V. S. R., and Murtugudde, R.: Variability, trend and controlling factors of Ocean acidification over Western Arabian Sea upwelling region, Mar. Chem., 209, https://doi.org/10.1016/j.marchem.2018.12.002, 2019.

https://doi.org/10.5194/egusphere-2026-3223
Preprint. Discussion started: 6 July 2026

Sridevi, B. and Sarma, V. V. S. S.: Role of river discharge and warming on ocean acidification and pCO2 levels in the Bay of Bengal, Tellus B Chem. Phys. Meteorol., 73, 1–20, https://doi.org/10.1080/16000889.2021.1971924, 2021.

Swierczek, S., Mazloff, M. R., and Russell, J. L.: Investigating Predictability of DIC and SST in the Argentine Basin Through Wind Stress Perturbation Experiments, Geophys. Res. Lett., 48, e2021GL095504, https://doi.org/10.1029/2021GL095504, 2021.

Szekely, T., Gourrion, J., Pouliquen, S., and Reverdin, G.: The CORA 5.2 dataset for global in situ temperature and salinity measurements: Data description and validation, Ocean Science, 15, https://doi.org/10.5194/os-15-1601-2019, 2019.

Tang, W., Fore, A., Yueh, S., Lee, T., Hayashi, A., Sanchez-Franks, A., Martinez, J., King, B., and Baranowski, D.: Validating SMAP SSS with in situ measurements, Remote Sens. Environ., 200, https://doi.org/10.1016/j.rse.2017.08.021, 2017.

Thadathil, P., Muraleedharan, P. M., Rao, R. R., Somayajulu, Y. K., Reddy, G. V., and Revichandran, C.: Observed seasonal variability of barrier layer in the Bay of Bengal, J. Geophys. Res. Oceans, 112, https://doi.org/10.1029/2006JC003651, 2007.

Thadathil, P., Thoppil, P., Rao, R. R., Muraleedharan, P. M., Somayajulu, Y. K., Gopalakrishna, V. V., Murthugudde, R., Reddy, G. V., and Revichandran, C.: Seasonal variability of the observed barrier layer in the Arabian Sea, J. Phys. Oceanogr., 38, https://doi.org/10.1175/2007JPO3798.1, 2008.

Thangaprakash, V. P., Girishkumar, M. S., Suprit, K., Suresh Kumar, N., Chaudhuri, D., Dinesh, K., Kumar, A., Shivaprasad, S., Ravichandran, M., Farrar, J. T., Sundar, R., and Weller, R. A.: What controls seasonal evolution of sea surface temperature in the Bay of Bengal?: Mixed layer heat budget analysis using moored buoy observations along 90°E, Oceanography, 29, https://doi.org/10.5670/oceanog.2016.52, 2016.

Twelves, A. G., Goldberg, D. N., Holland, P. R., Henley, S. F., Mazloff, M. R., and Jones, D. C.: Chlorophyll Production in the Amundsen Sea Boosts Heat Flux to Atmosphere and Weakens Heat Flux to Ice Shelves, J. Geophys. Res. Oceans, 129, e2024JC021121, https://doi.org/10.1029/2024JC021121, 2024.

Valsala, V. and Maksyutov, S.: Simulation and assimilation of global ocean pCO2 and air-sea CO2 fluxes using ship observations of surface ocean pCO2 in a simplified biogeochemical offline model, Tellus B Chem. Phys. Meteorol., 62, https://doi.org/10.1111/j.1600-0889.2010.00495.x, 2010.

Verdy, A. and Mazloff, M. R.: A data assimilating model for estimating Southern Ocean biogeochemistry, J. Geophys. Res. Oceans, 122, 6968–6988, https://doi.org/10.1002/2016JC012650, 2017.

Vinayachandran, P. N. and Kurian, J.: Hydrographic observations and model simulation of the Bay of Bengal freshwater plume, Deep. Sea. Res. 1. Oceanogr. Res. Pap., 54, https://doi.org/10.1016/j.dsr.2007.01.007, 2007.

Vinayachandran, P. N., Murty, V. S. N., and Babu, V. R.: Observations of barrier layer formation in the Bay of Bengal during summer monsoon, J. Geophys. Res. Oceans, 107, SRF 19-1, https://doi.org/10.1029/2001JC000831, 2002.

Vinayachandran, P. N., Das, U., Shankar, D., Jahfer, S., Behara, A., Nair, T. M. B., and Bhat, G. S.: Maintenance of the southern Bay of Bengal cold pool, Deep. Sea. Res. 2. Top. Stud. Oceanogr., 179, https://doi.org/10.1016/j.dsr2.2019.07.012, 2020.

https://doi.org/10.5194/egusphere-2026-3223
Preprint. Discussion started: 6 July 2026

Vinayachandran, P. N. M., Masumoto, Y., Roberts, M. J., Huggett, J. A., Halo, I., Chatterjee, A., Amol, P., Gupta, G. V. M., Singh, A., Mukherjee, A., Prakash, S., Beckley, L. E., Raes, E. J., and Hood, R.: Reviews and syntheses: Physical and biogeochemical processes associated with upwelling in the Indian Ocean, Biogeosciences, 18, 5967–6029, https://doi.org/10.5194/BG-18-5967-2021, 2021.

Wanninkhof, R.: Relationship between wind speed and gas exchange over the ocean, J. Geophys. Res., 97, https://doi.org/10.1029/92JC00188, 1992.

Wiggert, J. D., Murtugudde, R. G., and Christian, J. R.: Annual ecosystem variability in the tropical Indian Ocean: Results of a coupled bio-physical ocean general circulation model, Deep Sea Research Part II: Topical Studies in Oceanography, 53, 644–676, https://doi.org/10.1016/J.DSR2.2006.01.027, 2006.